Emergo
Studies in the Biogeophysical Environment

This technical description is from 2003. A few changes have been made to the model since then. For an update, please check the 'Changes from earlier versions' document on the MACRO homepage.

MACRO 5.0. A model of water flow and solute transport in macroporous soil. Technical description.

Mats Larsbo and Nicholas Jarvis

Swedish University of Agricultural Sciences
Department of Soil Sciences
Division of Environmental Physics

Emergo 2003:6
Report
ISSN 1651-7210
ISBN 91-576-6592-3

Abstract

This report presents a detailed technical description of version 5.0 of MACRO, a one-dimensional non-steady state model of water flow and solute transport in structured or macroporous field soils. A complete water balance is considered in the model, including treatments of precipitation (rain, snowpack and irrigation), variably-saturated water flow, losses to primary and secondary field drainage systems, evapotranspiration and root water uptake. Version 5.0 of MACRO can be used to simulate non-reactive tracers (e.g. bromide), tritium and pesticides including a single metabolite. The model includes descriptions of processes such as canopy interception and washoff, convective-dispersive solute transport with 'two-site' (kinetic and instantaneous) sorption, first-order degradation controlled by soil moisture and temperature conditions and plant uptake.

The model is run in two flow domains: a high-conductivity/low porosity macropore domain is coupled to a low-conductivity/high porosity domain representing the soil matrix. Mass exchange between the domains is calculated with approximate, physically-based, first-order expressions. The model structure therefore enables quantitative evaluation of the impact of macropore flow on solute transport in structured soils.

Contents

1. Introduction, 1

2. Conceptual basis and main features, 2

3. Driving variables, 3

4. Canopy processes, 4

4.1. Crop development, 4
4.2. Potential evapotranspiration, 5
4.3. Interception and canopy evaporation, 8

5. Soil water flow, 10

5.1. Hydraulic properties, 10
5.2. Source-sink terms, 18
5.3. Numerical solution, 23

6. Solute leaching and turnover, 28

6.1. Source-sink terms, 29
6.2. Discretisation of the convection-dispersion equation, 32
6.3. Boundary conditions, 33

7. Soil temperature, 34

7.1. Numerical solution, 35
7.2. Boundary conditions, 35

8. Acknowledgements, 36

9. References, 36
List of symbols, 43

1. Introduction

There is today increasing concern over the diffuse pollution threat to surface and groundwaters posed, for example, by the use of agricultural chemicals (e.g. fertilizers, pesticides). In this respect, the soil unsaturated zone acts as a critical buffer to solute transport and thus determines the risk of contamination of receiving water bodies by diffuse pollutants. Until recently, the prevailing conceptual model of water flow through soils was based on the idea that 'new' incoming water displaced existing 'old' water uniformly, with infiltrating water moving downwards in the soil profile behind a broad and well-defined 'wetting front'. Similarly, the prevailing view of solute transport was that leaching took place as a 'chromatographic' process, with the chemical as fully exposed to adsorption sites in undisturbed field soils as it would be both in laboratory batch experiments on water-slurry mixtures, or in column leaching experiments on repacked soils. The idea that water flow and chemical transport normally takes place as a uniform displacement process in soils has now been abandoned, and has been replaced by an understanding that the heterogeneity of undisturbed soils in the field often leads to markedly non-uniform patterns of water flow and solute displacement. The term preferential flow is used to describe this irregular wetting. It is a generic term, covering several processes with different physical causes, but with the common feature that non-uniform wetting leads to an increase in the effective velocity of the water flow through a small portion of the soil unsaturated zone. For example, countless experiments have shown that soil macropores (i.e. structural features such as root and earthworm channels, dessication cracks) allow rapid non-equilibrium fluxes of water to considerable depth in the soil profile (Beven & Germann, 1982). Preferential flow can also occur in the matrix of non-structured sandy soils due to water repellency (Ritsema et al., 1993), air entrapment and/or hysteresis (Nieber, 1996), and the presence of both large- and small-scale heterogeneities, such as soil layering and lenses of differing texture (Kung, 1990).

Flury et al. (1994) showed using dye tracing techniques that preferential flow is a widespread process, occurring in thirteen out of the fourteen investigated soils. Indeed, preferential flow has been widely demonstrated under field conditions, with contaminants such as pesticides detected in tile drain outflow or lysimeter outflows within weeks or even days of application and/or after only small amounts of accumulated drainage (e.g. Kladivko et al., 1991; Steenhuis & Parlange, 1991; Flury, 1996; Larsson & Jarvis, 1999a). Thus, preferential flow and transport in the unsaturated zone dramatically influences the leaching of surface-applied contaminants to groundwater, largely because the biologically active and chemically reactive topsoil is quickly by-passed (Jarvis, 2002).

This report presents a technical description of MACRO, a comprehensive mechanistic model of water and solute transport in field soils. The primary objectives behind the development of the MACRO model were to i.) synthesize current understanding of flow and transport processes in structured soils and ii.) develop an easy-to-use physically-based simulation model which could be used as a management tool to evaluate the likely impacts of macropore flow on water flow and solute transport to surface and groundwaters. Jarvis (1991) and Jarvis (1994) presented earlier versions of the MACRO model. MACRO has been widely applied since its first release, both in the research arena (e.g. Villholth & Jensen, 1998; Larsson & Jarvis, 1999a,b; Larsson & Jarvis, 2000; Jarvis et al., 2000; Kätterer et al., 2001) and in recent years in pesticide regulation in the EU (FOCUS, 1995; Jarvis, 1998). However, a number of limitations in the earlier versions of the model, especially with respect to the numerical solution methods, prompted the development of an entirely revamped model code, financed by the EU 5th framework projects APECOP and PEGASE. This report describes this latest Windows-based version (5.0) of the model, released in 2003.

2. Conceptual basis and main features

MACRO is a one-dimensional model that considers non-steady state fluxes of water, heat and solute for a variably-saturated layered soil profile. MACRO is a dual-permeability model, whereby the total soil porosity is partitioned into two separate flow regions (micropores and macropores), each characterized by a degree of saturation, conductivity, water flow rate, solute concentration, and solute flux density.

A full water balance is simulated, including treatments of precipitation (rainfall, irrigation and snow), evapotranspiration and root water uptake, deep seepage and horizontal fluxes to tile drains. With respect to solute transport and transformations, descriptions of processes such as convective-dispersive transport, canopy interception and washoff, sorption, biodegradation and plant uptake are included. A brief summary of some of the more important processes in the model is presented in Table 1. These processes are described in more detail in sections 4 to 7.

The complex flow pattern inherent in dual-permeability models represents a difficult numerical problem (Ray et al., 1997). A stable and robust solution is obtained in MACRO by decoupling calculations in the computer program with respect to the flow domains. Vertical water and solute fluxes are first calculated in the micropores. Updated values of water storages are used to determine the excess amount of water routed to the macropores. Water fluxes originating in the macropores are then

calculated and the solute concentrations in both domains which solve the solute balance are derived. Up to computational 200 layers are allowed, which ensures a high degree of numerical accuracy. Fully implicit solutions are used throughout which gives fast execution times despite a large number of potentially very thin computational layers. The various numerical procedures used in the MACRO model are described in more detail in sections 5.3, 6.2 and 7.1.

Table 1. Treatment of flow and transport processes in the MACRO model

Process	Treatment
Unsaturated water flow	Richards' equation in micropores, gravity flow in macropores
Root water uptake	Empirical sink term, water preferentially extracted from macropores
Seepage to drains and groundwater	Seepage potential theory. Sink term in vertical water flow equations
Solute transport	Convection/dispersion equation in the micropores, mass flow only in the macropores
Mass exchange	Approximate first-order rate equations for mass exchange of both solute and water
Sorption	Instantaneous equilibrium/kinetic sorption according to the ‘two-site’ model, Freundlich isotherm, sorption partitioned between micro- and macropores.
Degradation	first-order kinetics, separate rate coefficients for four pools (solid and liquid, micro- and macropores)
Soil temperature	Heat conduction equation

3. Driving variables

Driving variables in the model consist of measured precipitation data at a given constant solute concentration, daily maximum and minimum (or mean) air temperatures and either pre-calculated daily potential evapotranspiration data or additional meteorological variables required to calculate evapotranspiration internally in the model (solar radiation, wind speed and vapour pressure).

Either hourly or daily precipitation data may be used as input. In the former case, the precipitation is assumed to be evenly distributed during the one hour period. In the latter case, the user specifies an intensity (constant for the whole simulation period) so that the daily total can be distributed over a calculated duration, starting at midnight. The user may specify separate correction factors for rainfall and snow to account for wind drift losses in the measurements. Precipitation is partitioned into snow and rain depending on the air temperature. If the mean daily air temperature is above 2^{o}C then all the precipitation is assumed to fall as rain. If the temperature is less than -2^{o}C, then all the precipitation is assumed to be snow. The respective fractions falling as rain and snow are assumed to vary linearly between temperatures of -2 and +2^{o}C. Snowfall is added to a 'water-equivalent' pool, and losses due to snowmelt are calculated on a daily basis as a linear function of mean daily air temperatures above zero.

Irrigation may also be treated separately from natural precipitation. The model user specifies irrigation dates and times, application amounts, the solute concentration(s) in the applied water, and the fraction of the applied amount which is intercepted by the canopy. A separate treatment of irrigation and precipitation interception (section 4.3) allows the model user flexibility when simulating different types of irrigation application with widely varying interception losses (e.g. overhead sprinkler, raingun, fine pesticide sprays, surface flooding) and/or differing solute concentrations.

Daily potential evapotranspiration is required by the model. This is either supplied by the user as pre-calculated driving data, or is calculated internally using the Penman-Monteith equation from meteorological data (wind speed, solar radiation, vapour pressure and temperature). Evaporative demand within the day is estimated assuming an even distribution over a daylength calculated from the known site latitude and the day number in the year.

4. Canopy processes

4.1. Crop development

Three options are available to the model user: no crop (i.e. bare soil), an annual crop or a perennial crop. A simple description of the development of an annual crop is used in the model, with the green and total leaf area indices, *GLAI* and *LAI*, given as a function of day number in the year. Prior to crop emergence and after harvest, the ground is assumed to be bare. A linear development phase is assumed

between crop emergence and a user-specified day number D_{min}. This linear phase will normally be only a short period for spring-sown annual crops, but is especially useful for describing the leaf area development of autumn-sown crops during the long slow-growth winter period. Thereafter, between D_{min} and the day of maximum leaf area D_{max}, green leaf area index is given as :

$$GLAI = GLAI_{\min} + \left(GLAI_{\max} - GLAI_{\min}\right)\left(\frac{D^* - D_{\min}}{D_{\max} - D_{\min}}\right)^{x_1} \qquad (1)$$

where $GLAI_{max}$ and $GLAI_{min}$ are the maximum green leaf area and the value of $GLAI$ at D_{min} respectively, D^* is the current day number in the year and x_1 is an empirical `form' exponent. A similar expression is used to model the reduction in green leaf area between the maximum value and the day of harvest D_{harv} :

$$GLAI = GLAI_{harv} + \left(GLAI_{\max} - GLAI_{harv}\right)\left(\frac{D_{harv} - D^*}{D_{harv} - D_{\max}}\right)^{x_2} \qquad (2)$$

where $GLAI_{harv}$ is the green leaf area index at harvest and x_2 is an empirical exponent. The total leaf area LAI follows the development of green leaf area, except that it is maintained at the maximum value between D_{max} and D_{harv}. For an annual crop, root depth and crop height are assumed to increase in two linear phases from zero at crop emergence to a user-specified intermediate value at D_{min}, attaining maximum values at D_{max}. In the case of a perennial crop, the root depth, crop height and leaf area index are all assumed constant during the simulation.

4.2. Potential evapotranspiration

When the model user supplies meteorological data as driving variables, both the potential transpiration from cropped surfaces E_{p} and potential evaporation from the soil $E_{\text{p(soil)}}$ are calculated using the Penman-Monteith combination equation (Monteith, 1965) as a function of the crop surface resistance r_{c} and aerodynamic resistances from soil to canopy and from canopy to air (r_{ss} and r_{ca} respectively):

$$E_p = \frac{\left(\Delta F_{crop} R_n\right) + \left\{\rho C_p \left(\frac{VPD}{r_{ca}}\right)\right\}}{\lambda_v \left(\Delta + \gamma_c \left(1 + \frac{r_c}{r_{ca}}\right)\right)} \quad (3)$$

$$E_{p(soil)} = \frac{\left(\Delta F_{soil} R_n\right) + \left\{\rho C_p \left(\frac{VPD}{r_{ca} + r_{ss}}\right)\right\}}{\lambda_v \left(\Delta + \gamma_c\right)} \quad (4)$$

where λ_v is the latent heat of vapourization, Δ is the slope of the saturation vapour pressure vs. temperature curve, γ_c is the psychrometric 'constant', ρ and C_p are the density and specific heat capacity of air, *VPD* is the vapour pressure deficit and R_n is the net radiation calculated as:

$$R_n = R_i\left(1 - \alpha_r\right) - R_b \quad (5)$$

where R_i is the incoming solar radiation, α_r is the albedo and R_b is the outgoing long-wave radiation. The latter is calculated internally in the program as a function of air temperature and relative cloudiness, which, in turn, is estimated from the known daily solar radiation and site latitude. Beer's law is used to partition the net radiation into one fraction intercepted by the transpiring canopy surfaces F_{crop}, another fraction intercepted by dead plant material, and the remaining fraction which reaches the soil surface F_{soil} depending on the total and green leaf area indices:

$$F_{soil} = e^{-a_f LAI} \quad (6)$$

and

$$F_{crop} = 1 - e^{-a_f GLAI} \quad (7)$$

where a_f is the radiation attenuation factor. Surface resistance of the growing crop r_c is also calculated as a function of the green leaf area:

$$r_c = \frac{1}{GLAI\, k_s} \tag{8}$$

where k_s is the stomatal conductance, which in turn, is given as a function of the solar radiation R_i (in W m^{-2}) and vapour pressure deficit using the Lohammar equation (Lindroth, 1985):

$$k_s = \left(\frac{R_i}{R_i + R_{i(50)}} \right) \left(\frac{k_{s(\max)}}{1 + \frac{VPD}{VPD_{50}}} \right) \tag{9}$$

where $k_{s(max)}$ is the maximum stomatal conductance and $R_{i(50)}$ and VPD_{50} are the solar radiation and vapour pressure deficit at which conductance is reduced to 50% of the maximum value. The aerodynamic resistance from the canopy to the height of wind speed measurement r_{ca} is given from the well-known logarithmic wind profile:

$$r_{ca} = \frac{\left(\ln\left[\frac{z - d_h}{z_0} \right] \right)^2}{0.168 u(z)} \tag{10}$$

where u is the wind speed measured at height z above ground level and where the displacement height d_h and the roughness length z_0 are expressed as empirical functions of crop height H_c and leaf area index (Choudhury & Monteith, 1988):

$$d_h = 1.1 H_c \ln\left(1 + (0.2LAI)^{0.25}\right) \tag{11}$$

$$\begin{aligned} z_0 &= 0.0065 + \left(0.3 H_c (0.2LAI)^{0.5}\right) \quad ; \quad LAI < 1.0 \\ z_0 &= 0.3 H_c \left(1 - \left(\frac{d_h}{H_c}\right)\right) \quad ; \quad LAI \geq 1.0 \end{aligned} \tag{12}$$

The aerodynamic resistance from the soil surface to the canopy height r_{ss} is given as a function of crop height and wind speed using the exponential relationship suggested by Choudhury & Monteith (1988).

4.3. Interception and canopy evaporation

The treatment of precipitation interception by vegetation varies depending on both the crop type and form of precipitation. Clearly, if the ground surface is bare (either no crop at all, or an annual crop before emergence or after harvest), all precipitation is directly input to the soil. If the soil is cropped (either an annual crop during the growing season or a perennial) and the precipitation is natural rain, then all the water is assumed to be first diverted to the canopy, regardless of the degree of ground cover. If, on the other hand, the precipitation is in the form of irrigation, the amount of water diverted to the canopy is given `a priori' by the model user (see section 3.). This may vary from zero to 100% of the applied amount.

A running water balance is calculated for the canopy, with the inputs from rain and/or irrigation discussed above and losses by drip/throughfall and evaporation. Water diverted to the canopy is stored up to a maximum amount, the canopy interception capacity. For an annual crop, the interception capacity is assumed to increase linearly from zero at crop emergence to a user-specified maximum value at the maximum leaf area, returning to zero again at harvest. Water in excess of the canopy capacity immediately becomes effective net rainfall and enters the soil profile.

Canopy storage is emptied by evaporation. The potential wet canopy evaporation rate E_{wp} is expressed as:

$$E_{wp} = c_f E_p \tag{13}$$

where c_f is an empirical correction factor to account for enhanced evaporation loss from a wet canopy ($c_f \geq 1.0$). If the calculated value of E_{wp} is larger than the amount of water stored on the canopy W_c, then the wet canopy evaporation is set to the canopy storage and a potential root water uptake E_r is calculated as follows:

$$E_r = E_p - \left(\frac{W_c}{c_f} \right) \tag{14}$$

However, if the amount of water stored on the canopy is larger than the calculated value of E_{wp}, then the actual canopy evaporation rate equals the potential and root water uptake E_r is zero.

Net rainfall is characterized by a given solute concentration, the value of which is calculated differently in the model depending on whether a non-reactive tracer or pesticide transport is being simulated. Knowing the canopy water balance (see above), a running solute balance is updated at each time step. For the non-reactive case, the amount of solute on the canopy Q_c and the solute concentration c_t in the net rainfall are calculated assuming complete mixing:

$$Q_{c(t)} = \frac{W_c\left(Q_{c(t-\Delta t)} + \left(W_i\, c_p\right)\right)}{W_c + W_d} \tag{15}$$

and

$$c_t = \frac{\left(W_s\, c_p\right) + \left(W_d\left(\frac{Q_{c(t)}}{W_c}\right)\right)}{W_s + W_d} \tag{16}$$

where the subscript t refers to the current time step, W_i, W_s and W_d are the amounts of water intercepted by the canopy, directly striking the soil surface and reaching the soil as drip throughfall respectively and c_p is the solute concentration in the precipitation.

Processes of interception, dissipation and washoff of pesticides are treated in the same way as in the model PRZM (Carsel et al., 1984). Thus, with the same symbols as defined above for the non-reactive case, we have:

$$Q_{c(t)} = \left(W_i\, c_p\right) + \left(\frac{Q_{c(t-\Delta t)}\left(2 - \left(W_d\, f_e\right) - \left(\mu_c \Delta t\right)\right)}{\left(2 + \left(W_d\, f_e\right) + \left(\mu_c \Delta t\right)\right)}\right) \tag{17}$$

$$c_t = \frac{\left(W_s\, c_p\right) + \left(W_d\, f_e\, Q_{c(t-\frac{\Delta t}{2})}\right)}{W_s + W_d} \tag{18}$$

where Δt is the time step, f_e is an empirical foliar washoff coefficient (or 'extraction factor') and μ_c is a lumped dissipation rate coefficient including the effects of all loss processes (e.g. photolysis, volatilization).

5. Soil water flow

Richards' equation is used to calculate vertical water fluxes in the micropores:

$$C\frac{\partial \psi}{\partial t} = \frac{\partial}{\partial z}\left(K\left(\frac{\partial \psi}{\partial z} + 1\right)\right) - \sum S_i \qquad (19)$$

where $C = \partial\theta/\partial\psi$ is the differential water capacity, θ is the volumetric water content, ψ is the soil water pressure head, t is time, z is depth, K is the unsaturated hydraulic conductivity and S_i are source/sink terms for water exchange with macropores, drainage and root water uptake respectively.

The use of equation 19 to calculate water flows in the macropore domain is problematic due to the lack of information concerning $\psi(\theta)$ close to saturation. For this reason, capillarity is assumed to be negligible in the macropores, so that water flow is dominated by gravity (i.e. $d\psi/dz = 0$). The governing equation for water flow in macropores is then :

$$\frac{\partial \theta_{ma}}{\partial t} = \frac{\partial K_{ma}}{\partial z} - \sum S_i \qquad (20)$$

where θ_{ma} and K_{ma} are the macropore water content and hydraulic conductivity respectively. Since K_{ma} is assumed to be a power law function of θ_{ma} (section 5.1), this approach to describe water flow in macropores is equivalent to the kinematic wave approach to macropore flow described by Germann (1985).

5.1. Hydraulic properties

In macroporous soils, hydraulic conductivity increases very rapidly across a small pressure head range as saturation is approached (Clothier & Smettem, 1990; Jarvis & Messing, 1995). In MACRO, this macropore/micropore dichotomy is dealt with using a 'cut and join' approach to defining the hydraulic functions (Jarvis, et al. 1991; Wilson et al. 1992; Mohanty et al., 1997). A user-defined 'breakpoint' or 'boundary' pressure head (ψ_b) partitions the total porosity into micro- and macroporosity, while a corresponding water content (θ_b) and hydraulic conductivity (K_b) represent the saturated state of the soil matrix.

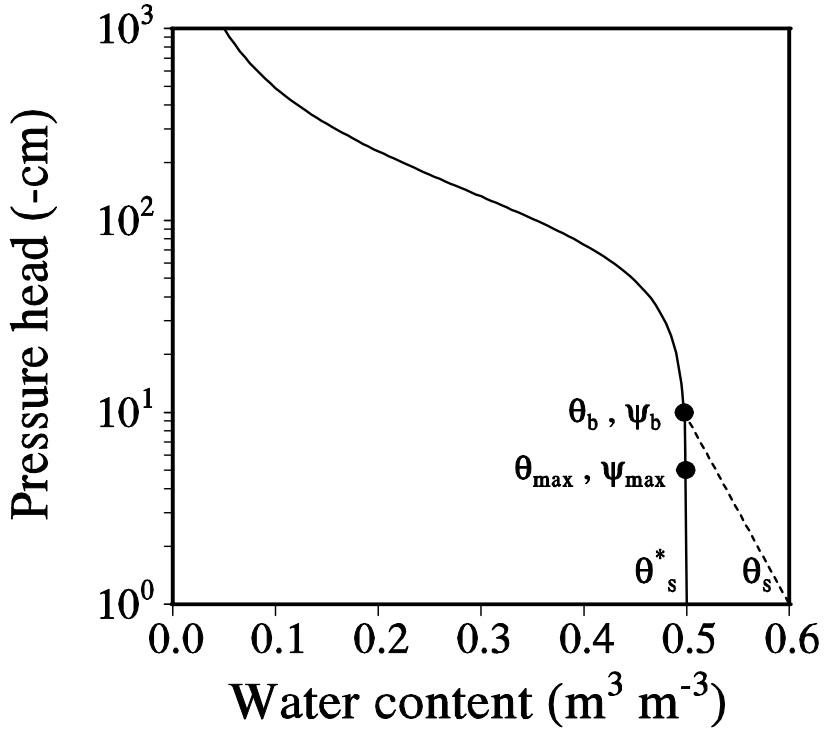

Fig.1. Modified van Genuchten soil water retention function used in MACRO5.0 (α_{vg} = 0.01 cm^{-1}, n_{vg} = 2, θ_r = 0.0 and θ^*_s = 0.5 m^3 m^{-3}).

Soil water retention in the micropores is calculated using a modified form of van Genuchten's (1980) equation (Fig.1):

$$S = \frac{\theta_{mi} - \theta_r}{\theta_s^* - \theta_r} = \left(1 + \left(\alpha_{vg}\psi\right)^{n_{vg}}\right)^{-m_{vg}} \qquad (21)$$

where S is an effective water content, m_{vg}, n_{vg} and α_{vg} are shape parameters (where m_{vg} is fixed equal to 1-1/n_{vg}), θ_r is the residual water content and θ_s^* is a 'fictitious' saturated water content, obtained by fitting equation 21 to retention data for pressure

heads less than ψ_b. It should be noted that θ_s^* does not represent the actual saturated water content in the model, as this is seperately defined by the user to reflect the macroporosity. Rather, it is only used internally in the program to extend the retention curve to pressure head values larger than ψ_b to allow for temporary oversaturation in the micropores when solving equation 19 (see section 5.3.1.5.).

Mualem's (1976) model is used to describe the unsaturated hydraulic conductivity function in the micropores, with the 'matching point' hydraulic conductivity given as K_b (Luckner et al., 1989):

$$K_{mi} = K_b \left(\frac{S}{S_{mi(\theta_b)}} \right)^l \left[\frac{\left(1 - \left(1 - S^{1/m_{vg}} \right)^{m_{vg}} \right)}{\left(1 - \left(1 - S_{mi(\theta_b)}{}^{1/m_{vg}} \right)^{m_{vg}} \right)} \right]^2 \tag{22}$$

where l is the tortuosity factor in the micropores, and $S_{mi(\theta b)}$ is given by:

$$S_{mi(\theta_b)} = \left(1 + \left(\alpha_{vg} \psi_b \right)^{n_{vg}} \right)^{-m_{vg}} \tag{23}$$

The hydraulic conductivity function in the macropores is given as a simple power law expression of the macropore degree of saturation S_{ma} :

$$K_{ma} = K_{s(ma)} S_{ma}^{n^*} \tag{24}$$

where n* is a 'kinematic' exponent reflecting macropore size distribution and tortuosity, and:

$$S_{ma} = \frac{\theta_{ma}}{e_{ma}} \tag{25}$$

where θ_{ma} is the macropore water content and e_{ma} is the macroporosity equivalent to the total saturated water content θ_s minus θ_b. It is recognized that macroporosity and macropore hydraulic conductivity may not be constant, but instead vary due to swelling and shrinkage. To account for this, simple relationships are assumed (Messing & Jarvis, 1990):

$$e_{ma} = e_s + p\left(\theta_b - \theta_{mi}\right) \tag{26}$$

$$K_{s(ma)} = \left(K_{s(\min)} - K_b\right)\left(\frac{e_{ma}}{e_s}\right)^{m^*} \tag{27}$$

where p is the slope of the shrinkage characteristic, e_s is the minimum value of macroporosity given by θ_s - θ_b, $K_{s(min)}$ is the minimum saturated hydraulic conductivity of a swelling soil attained when $e_{ma} = e_s$, and m^* is an empirical exponent.

5.1.1 Tillage effects on soil physical and hydraulic properties

In addition to swell/shrink, the topsoil structure is also changed by tillage, which is carried out to achieve favourable crop growth conditions. These sudden and dramatic changes are then slowly reversed by natural and traffic-induced consolidation of the soil. Tillage influences the flow paths for water and solutes and thus the risk of leaching of solutes to groundwater or surface waters (Brown et al., 1999; Jarvis, 2002). A simple physico-empirical sub-model of the effects of soil tillage on temporal changes in soil physical and hydraulic properties is included in MACRO5.0, and this is described in the following sections.

5.1.1.1. Phase relations

Tillage is assumed to change the bulk density and thereby the porosity and thickness of the ploughed layer. A simple way of modelling the changes in bulk density was proposed by Williams et al (1984) and is also used in the Root Zone Water Quality Model (Rojas & Ahuja, 1999), where the change is dependent on the state of the soil at tillage. A slightly modified version of their model is used:

$$\gamma^t = \gamma^{t-1} - I\left(\gamma^{t-1} - \gamma_{tilled}\right) \tag{28}$$

where γ is the soil bulk density, the index t denotes after tillage, t-1 before tillage, γ_{tilled} is the minimum bulk density and I is a tillage intensity factor varying between 0 and 1 depending on the type of implement. The total porosity, ε, can then be calculated from γ_{solid}, the particle density:

$$\varepsilon = 1 - \frac{\gamma}{\gamma_{solid}} \tag{29}$$

The relative change in microporosity is not necessarily the same as the relative change in total porosity. Thus, the microporosity after tillage, e_{mi}^{t}, is given by:

$$e_{mi}^{t} = e_{mi}^{t-1} + I\left(e_{mi(tilled)} - e_{mi}^{t-1}\right) \tag{30}$$

where $e_{mi(tilled)}$, is the microporosity attained immediately after tillage. The macroporosity e_{ma} is then:

$$e_{ma} = \varepsilon - e_{mi} \tag{31}$$

The saturated micropore water content is given as the microporosity minus the trapped air porosity. The change in the trapped air volume is assumed to be proportional to the change in microporosity.

Tillage is assumed to completely mix the solid, solute, water and heat contents from the surface to the depth of ploughing. The thermal properties are then updated for the bulk densities and water contents after tillage using the procedures described in section 7.

5.1.1.2. Micropore hydraulic properties

Apart from the total pore volume, it is assumed that only the α_{vg}-value in the van Genuchten equation, which reflects a characteristic micropore size, is changed at tillage. A new van Genuchten retention curve (Fig. 2) using the same residual water content and n_{vg}-value is fitted to the actual saturated micropore water content calculated from equation 30. This concept is similar to classical Miller scaling (Miller & Miller, 1956). The micropore hydraulic conductivity function can be expressed as (Hoffmann-Riem et al., 1999):

$$K_{mi} = k_0\left(\theta_b - \theta_r\right)S^l\alpha_{vg}{}^2\left[1-\left(1-S^{1/m_{vg}}\right)^{m_{vg}}\right]^2 \tag{32}$$

where k_0 is a coefficient of proportionality, assumed to be independent of the consolidation state of the soil. Since the saturated micropore conductivity and the α_{vg}-value in a fully consolidated soil are model parameters, k_0 can be calculated from equations 21 and 32 with ψ replaced by ψ_b. The maximum saturated micropore conductivity attained after tillage, is also given as a parameter in the model. Again, equations 21 and 32 with $\theta_b=\theta_{b(tilled)}$, can be solved numerically for

$\alpha_{vg(tilled)}$, the maximum α_{vg}-value. The temporal changes in the retention curve induced by tillage then follow from:

$$\alpha_{vg}^{t} = \alpha_{vg}^{t-1} + I\left(\alpha_{vg(tilled)} - \alpha_{vg}^{t-1}\right) \tag{33}$$

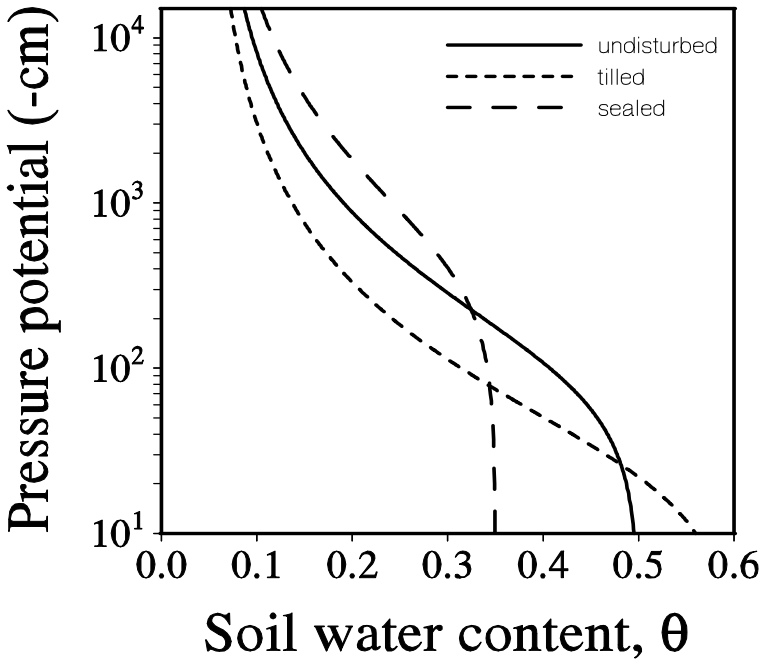

Fig. 2. Schematic sketch of van Genuchten retention curves for three different states of the topsoil.

5.1.1.3. Macropore hydraulic properties

The change in unsaturated macropore conductivity is calculated in the same way as for shrinkage induced changes of the macroporosity (see equation 27):

$$K_{s(ma)} = \left(K_{s(cons)} - K_{b(cons)}\right)\left(\frac{e_{ma}}{e_{ma(cons)}}\right)^{m^*} \tag{34}$$

where $K_{s(cons)}$ is the saturated conductivity in a fully consolidated soil, $K_{b(cons)}$ is the saturated micropore conductivity in a fully consolidated soil and $e_{ma(cons)}$ is the macroporosity in a fully consolidated soil.

Ploughing cuts the macropores and thereby changes the preferential flow paths. This effect on the continuity of macropores is modelled as an increase in the macropore size distribution index:

$$n^{*t} = n^{*t-1} + I\left(n^{*}_{tilled} - n^{*t-1}\right) \tag{35}$$

where n^{*}_{tilled} is the maximum value of the macropore size distribution index.

5.1.1.4. Consolidation and surface sealing

For the sake of simplicity, it is assumed that only the amount of rain reaching the soil surface determines the quasi-continuous consolidation and surface sealing of the soil. It is also assumed that topsoil layers below the depth of tillage consolidate by a user-defined percentage on each tillage occasion due to traffic induced compaction, providing they are not already fully consolidated. This simple empirical approach is justified by the fact that the model is not intended to facilitate study of consolidation and surface sealing as such, but rather their effects on water flow and solute transport.

Surface sealing is modelled in the same way as natural consolidation. Sealing, however, only affects a thin layer at the soil surface and the rate of consolidation is usually much higher. Consolidation due to rain is modelled with a first-order rate expression. The bulk density the macroporosity, the macropore distribution index and the α_{vg}-value are all assumed to consolidate in the same manner. The equation for bulk density consolidation is given here as an example:

$$\frac{d\gamma}{dR_{amount}} = k_{cons}\left(\gamma_{cons} - \gamma\right) \tag{36}$$

where R_{amount} is the accumulated rain amount, k_{cons} is a consolidation rate constant and γ_{cons} is the bulk density in a fully consolidated soil. Different values of k_{cons} and γ_{cons} are used for simulating surface seal development and topsoil consolidation following tillage. Solving equation 36 for γ gives (see Fig.3):

$$\gamma = \gamma_{cons} - e^{\left[\ln\left(\gamma_{cons} - \gamma_{tilled}\right) - k_{cons}R\right]} \tag{37}$$

From equations 32 and 34, it can be seen that the consolidation effects on the saturated conductivity and the saturated micropore conductivity will not follow equation 37. For bulk density, macroporosity, the macropore size distribution index

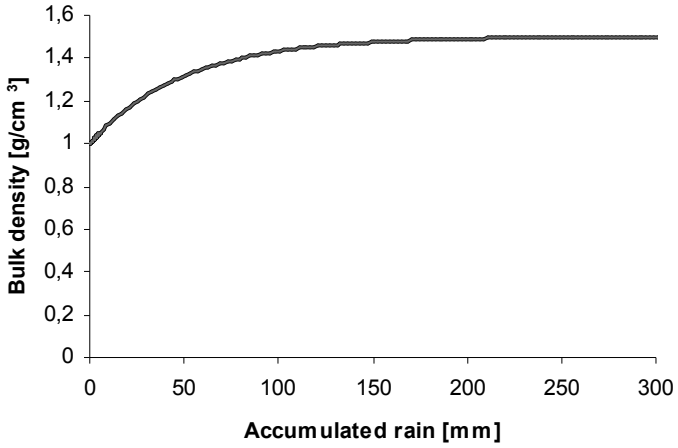

Fig. 3. Consolidation with γ_{tilled}=1 g cm^{-3}, γ_{cons}=1.5 g cm^{-3} and k_{cons}=0.02 mm^{-1}

and α_{vg}, initial values are determined as a percentage of the difference between the tilled and fully consolidated state by the parameter C_{init}. For example, the initial bulk density γ_{init} is given by:

$$\gamma_{init} = \gamma_{tilled} + \left(0.01 \cdot C_{init}\right) \cdot \left(\gamma_{cons} - \gamma_{tilled}\right) \tag{38}$$

5.1.1.5. Aggregate size

Exchange of water and solutes between macropores and micropores is strongly affected by the geometry and size of soil aggregates (Gerke & van Genuchten, 1996), and also the properties of aggregate skins ('cutans') or macropore surfaces (Gerke & Köhne, 2002). In MACRO, these mass exchange processes are modelled using the concept of an 'effective' diffusion pathlength, described in more detail in sections 5.2.1 and 6.1.2. Since the effective diffusion pathlength reflects soil aggregate structure, it is likely to be strongly affected by tillage. However, tillage is assumed to change the diffusion pathlength in a way that is not likely to be consistent with the tillage intensity concept used for other physical and hydraulic properties (see equation 28). Therefore, the effective diffusion pathlength attained immediately after each tillage occasion is treated as a user-defined parameter. The effect of subsequent consolidation on the diffusion pathlength is modelled as a first-order function of rainfall, in the same way as for the other physical parameters.

5.2. Source-sink terms

5.2.1. Water exchange between macropores and micropores

In the absence of gravity, Richards equation can be recast as a diffusion equation, with gradients in water content as the driving force. In MACRO, water uptake from macropores by unsaturated micropores is treated as a first-order approximation to this water diffusion equation, assuming a rectangular-slab geometry for the aggregates (Booltink et al., 1993; van Genuchten & Dalton, 1986; Šimůnek et al., 2003):

$$S_w = \left(\frac{G_f \; D_w \gamma_w}{d^2} \right) \left(\theta_b - \theta_{mi} \right) \tag{39}$$

where d is an effective 'diffusion' pathlength related to aggregate size and the influence of coatings on macropore and aggregate surfaces, D_w is an effective water diffusivity, G_f is a geometry factor (set internally to 3 for a rectangular slab geometry, van Genuchten, 1985; Gerke & van Genuchten, 1996) and γ_w is a scaling factor introduced to match the approximate and exact solutions to the diffusion problem (van Genuchten, 1985; Gerke & van Genuchten, 1993; Jarvis, 1994). The scaling factor γ_w varies with the initial water content and hydraulic properties, but not strongly (see Gerke & van Genuchten, 1993; Jarvis, 1994), so that for simplicity and convenience, γ_w is set within the program to an average value (Jarvis, 1994). The effective water diffusivity is assumed to be given by:

$$D_w = \left(\frac{D_{\theta_b} + D_{\theta_{mi}}}{2} \right) S_{ma} \tag{40}$$

where $D_{\theta b}$ and $D_{\theta mi}$ are the water diffusivities at the saturated micropore water content and the current micropore water content respectively and where S_{ma} is introduced to account for incomplete wetted contact area between the two pore domains. In the Mualem/van Genuchten model, $D_{\theta mi}$ is given as (van Genuchten, 1980):

$$D_{\theta mi} = \left[\frac{\left(1 - m_{vg}\right) K_s^*}{\alpha_{vg} \, m_{vg} \left(\theta_s^* - \theta_r \right)} \right] S^{l - 1/m_{vg}} \left[\left(1 - S^{1/m_{vg}} \right)^{-m_{vg}} + \left(1 - S^{1/m_{vg}} \right)^{m_{vg}} - 2 \right] \tag{41}$$

where K_s^* is a 'fictitious' saturated hydraulic conductivity obtained by extrapolating the micropore conductivity function to zero pressure head:

$$K_s^* = K_b \left(\frac{1}{S_{mi(\theta_b)}} \right)^l \left(1 - \left(1 - S_{mi(\theta_b)}^{\ 1/m_{vg}} \right)^{m_{vg}} \right)^{-2} \quad (42)$$

and $D_{\theta b}$ is given by setting S in equation 41 to $S_{mi(\theta b)}$ (see equation 23).

Equation 39 only describes flow from macropores to micropores and not in the reverse direction. Flow from micropores to macropores occurs instantaneously (i.e. within one time step), if the micropore water content exceeds θ_b (i.e. ψ exceeds ψ_b), following the basic physical principle that governs the filling of pores when the water-entry pressure is exceeded. This can occur internally within the soil, or at the soil surface, when the rainfall rate exceeds the micropore infiltration capacity (section 5.3.1.2). Some numerical considerations concerning the transfer of excess water from micropores to macropores are discussed in section 5.3.1.5.

5.2.2. Drainage

Lateral water flow to seepage surfaces is calculated as a sink term in equation 19 describing vertical fluxes in the soil profile. The degree of saturation in the macropores defines the location and extent of saturated zones that contribute to drainflow. If the macropores are unsaturated, then no flow to drains occurs. If the macropores are saturated, then flow to drains will take place irrespective of the degree of saturation of the micropores. If the latter are unsaturated, then only the macropores contribute to the flow.

There are two situations where seepage fluxes are considered in the model. Firstly, flow to field drains is calculated when the tile drainage option is selected. The drains are assumed to be overlain by fully penetrating seepage surfaces (i.e. ditches or drains with highly permeable backfill). Secondly, groundwater seepage to a secondary drainage system (i.e. streams, canals, or perimeter field ditches) is calculated in the model as a means of regulating water table heights when the bottom boundary condition option accounting for a water table located in the profile is used. In both cases, flux rates from saturated layers above the drainage depth are predicted using seepage potential theory for layered soils (Youngs, 1980; Leeds-Harrison et al., 1986), so that the total drainage rate $q_{d(tot)}$ from a saturated zone is given by:

$$q_{d(tot)} = A_f E \quad (43)$$

where A_f is a shape factor and E is the seepage potential given by:

$$E = \int_{h_0}^{H} K(h)(H - h)\, dh \tag{44}$$

where $K(h)$ is the hydraulic conductivity varying with height h, h_0 is the height of the base of the saturated zone and H is the water table height. All heights are measured with respect to a datum at the base of the profile. For parallel field drains, the shape factor A_f is simply given by (Youngs, 1980):

$$A_f = \frac{8}{L^2} \tag{45}$$

where L is the drain spacing. For general groundwater seepage, the water table height is assumed to be controlled by seepage from a square-shaped drainage basin of known area A_d. The shape factor is then given by (Youngs, 1980):

$$A_f = \frac{13.652}{A_d} \tag{46}$$

Evaluating the integral in equation 44 gives the seepage potential e in each individual micropore and macropore domain in each layer of the saturated zone above drain depth as (Leeds-Harrison et al., 1986):

$$e = K\left(\left(H\, h_u - \frac{h_u^2}{2}\right) - \left(H\, h_l - \frac{h_l^2}{2}\right)\right) \tag{47}$$

and the drainage rate q_d for each such domain as :

$$q_d = A_f e \tag{48}$$

where h_u and h_l are the heights at the top and bottom of the layer and K is given by K_s minus K_b in the macropores and K_b in the matrix. In the layer in which the water table is located, h_u in equation 47 is replaced by H.

Water flow to drains from layers below the drainage depth q_{dd} is calculated using the first term of the well-known Hooghoudt drainage equation (Hooghoudt, 1940):

$$q_{dd} = \frac{8K d_z \left(H - D_z\right)}{L^2} \tag{49}$$

where D_z is the depth of soil between drain depth and the base of the simulated profile, and d_z is the equivalent or reduced depth of soil after accounting for radial flow resistances, given by:

$$d_z = \frac{D_z}{\left(\left(\left(\frac{8}{\pi}\ln\left(\frac{D_z}{u_p}\right)\right) - 3.4\right)\left(\frac{D_z}{L}\right)\right) + 1} \quad ; \qquad D_z \le 0.3L$$

$$d_z = \frac{\pi L}{8\left(\ln\left(\frac{L}{u_p}\right) - 1.15\right)} \quad ; \qquad D_z > 0.3L \tag{50}$$

where u_p is the wetted perimeter of the drain. Equation 49 gives the flow contribution from the entire depth of soil between drain depth and the bottom of the profile (i.e. an impermeable layer). In MACRO, this flow is partitioned between the numerical layers in proportion to the layer thicknesses.

5.2.3. Water uptake by roots

Root water uptake is calculated from evaporative demand, root distribution and soil water content using the simple empirical sink function described by Jarvis (1989). In this model, it is assumed that the ratio between actual and potential root water uptake (E_a/E_r) varies as a function of a dimensionless water stress index ω^*. A threshold-type function is assumed, such that the total stress must exceed a critical value of the water stress index ω^*_c (the`root adaptability factor') before transpiration is reduced (Fig. 4). Thus, the crop can adjust to stress in one part of the root system by increasing uptake from other parts where conditions may be more favourable (Jarvis, 1989).

The stress index is calculated by combining two functions describing the distribution of roots and water content in the soil profile:

$$\omega^* = \sum_{i=1}^{i=k} r_i \, \omega_i \tag{51}$$

where k is the number of soil layers in the profile containing roots and r_i and ω_i are the proportion of the total root length and a water stress 'reduction factor' in layer i respectively. Again, a threshold type of response is assumed for the reduction factor ω (Feddes et al., 1976), accounting for soil conditions that are either too wet or too dry (Fig. 5). Root water uptake is assumed to be reduced to zero both at the saturated water content θ_s and also at the extractable water content (i.e. wilting point) θ_w.

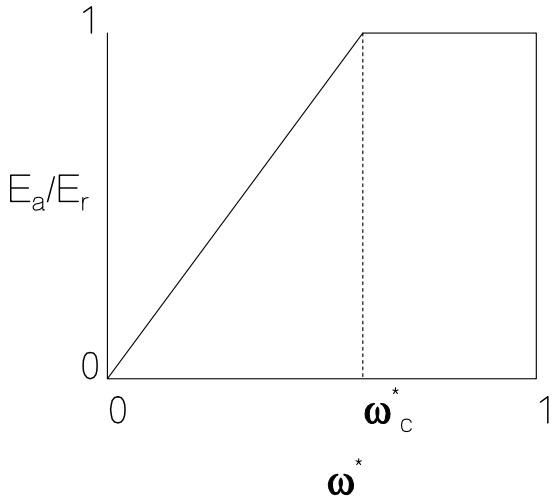

Fig. 4. Ratio of actual to potential transpiration as a function of the stress index ω^*

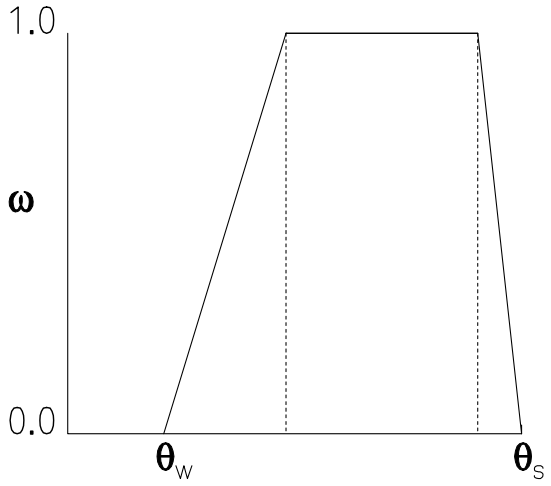

Fig.5. Soil water stress function for reduction of transpiration.

Root length is assumed to be distributed logarithmically with depth (Feddes et al., 1974; Gerwitz & Page, 1974):

$$r_i = \zeta \left(\frac{\Delta z_i}{z_r} \right) e^{-\zeta \left(\frac{z_{m(i)}}{z_r} \right)} \tag{52}$$

where Δz_i and $z_{m(i)}$ are the thickness and mid-point depth below the soil surface of layer i, z_r is the root depth and ζ is an empirical root distribution parameter. Finally, the total water uptake is distributed within the root depth according to the stress in each layer. The water uptake sink (S_r, see equation 19) is therefore given by:

$$S_r = \left(\frac{E_a}{\Delta z_i} \right) \left(\frac{r_i \omega_i}{\omega^*} \right) \tag{53}$$

The calculated uptake is preferentially extracted from water in the macropores. Any excess demand is then satisfied from water stored in the micropores.

5.3. Numerical solution

5.3.1. Water flow in micropores

5.3.1.1. Iteration procedure

The left-hand side in equation 19 can be approximated by:

$$C \frac{\partial \psi}{\partial t} = C_i^n \frac{\psi_i^{n+1} - \psi_i^n}{\Delta t} \tag{54}$$

where i is the spatial index, n is the temporal index and Δt is the time step. However, because of the explicit linearization of C, this approximation leads to an error in the mass balance given by:

$$Error_i = \left(\theta_i^{n+1} - \theta_i^n \right) - C_i^n \left(\psi_i^{n+1} - \psi_i^n \right) \tag{55}$$

To reduce this error an iterative solution is used (Celia et al., 1990):

$$\theta_i^{n+1} - \theta_i^n = C_i^{n+1,\tau} \left(\psi_i^{n+1,\tau+1} - \psi_i^{n+1,\tau} \right) + \theta_i^{n+1,\tau} - \theta_i^n \tag{56}$$

where τ denotes the iteration level. Richards equation (equation 19) can then be written in discrete form as:

$$C_i^{n+1,\tau}\left(\psi_i^{n+1,\tau+1}-\psi_i^{n+1,\tau}\right)+\theta_i^{n+1,\tau}-\theta_i^{n}= \tag{57}$$
$$\frac{\Delta t}{\Delta z_i}\left[K_{i-1/2}^{n}\left(\frac{\psi_{i-1}^{n+1,\tau+1}-\psi_i^{n+1,\tau+1}}{(\Delta z_{i-1}+\Delta z_i)/2}+1\right)-K_{i+1/2}^{n}\left(\frac{\psi_i^{n+1,\tau+1}-\psi_{i+1}^{n+1,\tau+1}}{(\Delta z_i+\Delta z_{i+1})/2}+1\right)\right]$$

where the K values between nodes are explicitly linearized and calculated using arithmetic means (van Dam, 2000). The first term on the left-hand side of equation 57 vanishes as the iterative scheme converges towards a perfect mass balance. In the first iteration, the values at time $n+1$ and iteration level 1 are assumed to be equal to the values at time n. The number of iterations required is determined by the tolerance criterion $abs\left(\theta_i^{n+1,\tau+1}-\theta_i^{n+1,\tau}\right)\le 0.000001$ when layer i is unsaturated and by $abs\left(\psi_i^{n+1,\tau+1}-\psi_i^{n+1,\tau}\right)\le 0.000001$ when layer i is saturated (van Dam, 2000). Convergence is usually fast and stricter criteria have little effect on the solution. If the solution does not fulfil the convergence criteria within 10 iterations, the time step used for solving Richards' equation is halved and the iterative scheme is resolved again. This procedure is repeated until the solution converges. The scheme is then repeatedly solved until these internal time steps sum up to the base time step in the model. If the internal time step decreases below 10^{-5} h Richards' equation is solved explicitly using a standard Euler method.

5.3.1.2. Surface boundary condition

Water will flow into surface-vented macropores if the rainfall intensity exceeds the infiltration capacity of the micropores. Thus, the net rainfall at the soil surface in a given time interval (= $W_s + W_d$, see section 4.3) is partitioned into soil evaporation E_s, an amount infiltrating into the micropores I_{mi} and an excess amount flowing into macropores I_{ma} depending on the micropore infiltration capacity I_{max} :

$$\begin{aligned} I_{mi} &= W_s + W_d - E_s \quad ; \quad W_s + W_d - E_s \le I_{max} \\ I_{ma} &= 0 \end{aligned} \tag{58}$$
$$\begin{aligned} I_{mi} &= I_{max} \quad ; \quad W_s + W_d - E_s > I_{max} \\ I_{ma} &= W_s + W_d - E_s - I_{mi} \end{aligned}$$

Thus, if the first condition in equation 58 is satisfied, then the top boundary condition is defined by a known flux (Neumann condition) equal to the net rainfall minus soil evaporation. If the second condition is satisfied, then the soil surface boundary condition is given by a known tension (Dirichlet condition). Changes from a known flux to a known tension and vice versa may occur between iterations.

The infiltration capacity $I_{\max}$ is given from Darcy's law as:

$$I_{\max} = K_{top}\left(\frac{\left(\psi_{b(1)} - \psi_1^{n+1}\right)}{\Delta z_1 / 2} + 1\right) \tag{59}$$

where the subscript *1* refers to the surface soil layer and K_{top} is given by the arithmetic mean of K_b and K for the surface layer. When the micropores are saturated, the infiltration capacity is simply given by K_b.

The soil evaporation rate E_s is calculated by comparing the potential loss $E_{p(soil)}$ (equation 4) with the maximum possible rate of supply of water to the soil surface $q_{\max}$ (Feddes et al., 1974):

$$E_s = \min.\left(q_{\max}, E_{p(soil)}\right) \tag{60}$$

where $q_{\max}$ is calculated iteratively by substituting Mualem-van Genuchten's model into Darcy's law and evaluating the flux as a function of the unknown pressure head at the surface and the known pressure head at the first node. The hydraulic conductivity is evaluated as an arithmetic mean of the conductivities at the two pressure heads.

5.3.1.3. Bottom boundary condition

There are four different options for the bottom boundary condition:

1. *Known hydraulic gradient* – the percolation is equal to the user defined hydraulic gradient times the unsaturated conductivity in the bottom layer.
2. *Known pressure head* – the pressure head at the bottom boundary is user defined. The pressure head can vary with time but must be negative.
3. *Groundwater table in the profile* – when the bottom soil layer is unsaturated, an upward directed hydraulic gradient exists and capillary rise into the profile is calculated assuming a zero pressure head at the base. When the bottom soil layer is saturated, the percolation q_{out} is calculated as a linear function of the water table height H:

$$q_{out} = q_{const}\left(\frac{K}{K_s}\right)H \qquad (61)$$

where q_{const} is an empirical parameter and K refers to the saturated hydraulic conductivity of either the macropore or micropore regions (i.e. K_b or K_s-K_b) in the deepest horizon of the profile. Thus, in this way, the percolation rates from the macropores and micropores are weighted by their relative hydraulic conductivities.

4. *Lysimeter* – the pressure head at the bottom boundary is set to zero but no upward flow is allowed.

Since the pressure heads in the numerical layers closest to the bottom boundary are not allowed to increase above ψ_b, for boundary conditions *2-4* there will be an artificial continuous upward flow when the distance between the centre of the numerical layer and the bottom of the profile, z_b, is less than the absolute value of ψ_b plus the pressure head at the bottom boundary. To solve this problem, ψ_b is automatically set equal to the pressure head at the bottom boundary minus z_b for the affected numerical layers at the base of the profile. This does not influence simulation results in any critical way since K_b and θ_b remain unchanged.

It can be deduced from equation 61 that for the seepage boundary condition, *3*, the criterion for convergence of the numerical solution to Richards' equation is:

$$\frac{q_{const}\,H}{K_s} \leq 1 \qquad (62)$$

This restriction in parameter values should not pose any problems with realistic parameterisations of the model.

5.3.1.4. Updating flows and storages

The numerical solution to Richards equation supplies updated pressure heads at each node, which are then used to update water storages in each layer from the known water retention function. Water flow rates in micropores are calculated from storage differences in each soil layer when either the surface or bottom boundary condition is of Neumann type. When both boundary conditions are of Dirichlet type, the flows are calculated from the known pressure heads using Darcy's law.

5.3.1.5. Hydraulic functions and the generation of macropore flow

As shown in Fig.1, the division between flow domains is defined by a pressure head ψ_b and the corresponding water content θ_b. If the micropore water content exceeds θ_b, the excess water will drain into the macropores. However, the macropores only have a fixed capacity to accept water, C_{ma}, equal to:

$$C_{ma} = (1 - S_{ma})(\theta_s - \theta_b) \tag{63}$$

Therefore, an additional breakpoint on the modified van Genuchten retention curve (θ_{max}, ψ_{max}, see Fig. 1) defines the maximum amount of excess water allowed in the micropores at each timestep, corresponding to C_{ma} (i.e. $\theta_{max} = \theta_b + C_{\mathrm{ma}}$). When solving Richards' equation, the pressure heads are allowed to increase above ψ_{max} only if the macropores are also saturated. In this situation, the water capacity is set to zero for pressures above ψ_{max}. For pressure heads above ψ_b, the micropore hydraulic conductivity is set to K_b. Once Richards' equation has been solved, all water exceeding θ_b is instantly removed from the micropores and added to the macropores.

The cutting of the retention curve close to saturation in the modified van Genuchten model shown in Fig.1 has consequences for the numerical solution to Richards' equation. Since the water capacity function becomes discontinuous, the iterative scheme (equation 57) is not guaranteed to converge. However, such convergence problems are very rare in simulations with realistic parameterisations.

The hydraulic conductivity function in the original van Genuchten model shows an abrupt increase close to saturation for n_{vg}-values close to 1. The introduction of $\psi_b<0$ means that this increase is less dramatic when micropore saturation is approached. Vogel et al. (2001) simulated infiltration with a modified van Genuchten model, using values for the 'minimum capillary height' (the exact equivalent to the boundary pressure head in MACRO) of a few centimetres. They concluded that convergence problems and oscillations in the numerical solutions for n_{vg}-values close to unity that occurred with the original van Genuchten model were efficiently removed by this approach.

5.3.2. Water flow in macropores

An implicit iterative technique called interval halving is used to solve the local water balance in the macropores for each layer, in turn, from the soil surface downwards. If the flow capacity of both micro- and macropores is exceeded in any layer, then the

local water balance cannot be solved (over-saturation develops in the macropores). In this situation, the excess water is added to the macropore storage in the layer(s) above, and water fluxes between layers are corrected accordingly. This approach, rather than the usual finite difference methods, was dictated by the simplifying assumption of gravity flow in macropores.

6. Solute leaching and turnover

Solute transport in micropores is calculated using the convection-dispersion equation with source/sink terms U_i to represent a wide range of different processes, including mass exchange between flow domains, kinetic sorption, solute uptake by the crop, biodegradation and lateral leaching losses to drains and/or regional groundwater:

$$\frac{\partial\left(c\theta_{mi(m)}+\left(1-f-f_{ne}\right)\gamma s\right)}{\partial t} = \frac{\partial}{\partial z}\left(D\,\theta_{mi(m)}\,\frac{\partial c}{\partial z} - qc\right) - \sum U_i \qquad (64)$$

where s is the sorbed concentration in the equilibrium pool, c is the solute concentration in the liquid phase, f is the mass fraction of the solid material in contact with water in the macropore domain, f_{ne} is the fraction of the solid material providing non-equilibrium (i.e. kinetic) sorption sites, $\theta_{mi(m)}$ is the mobile water content, accounting for an inaccessible soil volume due to anion exclusion, q is the water flow rate and D is the dispersion coefficient given by:

$$D = D_v\, v + D_o\, f^* \qquad (65)$$

where D_o is the diffusion coefficient in free water, f^* is the impedance factor which is calculated according to Millington and Quirk (1961), D_v is the dispersivity, and v is the pore water velocity. In the macropores, an equivalent approach is used to calculate transport, except that dispersion is not explicitly calculated and only equilibrium sorption is considered (i.e. D and f_{ne} are zero). Equilibrium sorption partitioning is calculated using the Freundlich isotherm:

$$s = k_f\, c^m \qquad (66)$$

where k_f is the sorption coefficient and m is the Freundlich exponent.

6.1. Source-sink terms

6.1.1. Kinetic sorption

Kinetic sorption is treated as a source-sink term to equation 64 following a 'two-site' approach described by Altfelder et al. (2000), where the kinetic sorption sites are assumed to respond to changes in the adsorbed concentration at the equilibrium sites:

$$U_k = \frac{\partial A_{ne}}{\partial t} = \alpha_k \left(\gamma s - \frac{A_{ne}}{f_{ne}} \right) \tag{67}$$

where A_{ne} is the mass of solute stored per unit soil volume at the kinetic sites and α_k is a first-order mass transfer coefficient.

6.1.2. Solute exchange between macropores and micropores

The source/sink term for mass transfer of solute between micro- and macropores U_e is given by a combination of a diffusion component and a mass flow component:

$$U_e = \left(\frac{G_f \; D_e \theta_{mi(m)}}{d^2} \right) \left(c_{ma} - c_{mi} \right) + S_w c' \tag{68}$$

where the prime notation indicates either the solute concentration in macropores or in 'accessible water' in the micropores, depending on the direction of water flow S_w (i.e. $c' = c_{ma}$ if water flows from the macropores to the micropores) and D_e is an effective diffusion coefficient approximated by:

$$D_e = D_o f^* S_{ma} \tag{69}$$

where, as before (see equation 40), S_{ma} is included to account for incomplete wetted contact area between the flow domains.

6.1.3. Solute loss to drains and groundwater

The loss of solute to the drains and to lateral groundwater seepage is calculated assuming complete mixing within a flow domain in the horizontal dimensions. Thus, the drainage sink term U_t to equation 64 is given by:

$$U_t = \frac{q_d}{\Delta z} c' \tag{70}$$

In addition to leaching losses to field drainage systems, solute loss/gain in lateral shallow groundwater flow U_g is calculated for each saturated soil layer using a retention time concept:

$$U_g = \theta \left(\frac{c' - c_g}{R_t} \right) \tag{71}$$

where R_t is the retention time. Depending on the solute concentration in the groundwater c_g, this term either adds or removes solute from the soil profile, but it does not alter the water balance, since steady-state lateral groundwater flow is implicitly assumed.

6.1.4. Root uptake and evaporative loss of solutes

The solute uptake rate by roots U_c is modelled as a passive process as a function of root water uptake and the solute concentration:

$$U_c = f_c S_r c' \tag{72}$$

where f_c is an empirical 'concentration factor' (Boesten & van der Linden, 1991). For tritium transport, f_c is set automatically to unity within the program. Tritium is also lost as water evaporated from the soil surface. This is treated as an additional sink term in equation 64 and is calculated as the bare soil evaporation rate E_s (equation 60) multiplied by the tritium concentration in the uppermost soil layer.

6.1.5. Degradation and pesticide metabolites

Degradation rates in each of four pools (two phases, liquid and equilibrium adsorbed, in each of two domains) are calculated using first-order kinetics with each pool characterized by separate reference rate coefficients μ_{ref}. The degradation rate in the kinetically-adsorbed pool can either be set equal to the degradation rate in the equilibrium pool or to zero. Actual degradation rate coefficients in the field μ are predicted from laboratory-measured reference values using functions F_w and F_t to account for the effects of soil moisture and temperature (Boesten & van der Linden, 1991):

$$\mu = \mu_{ref} F_w F_t \tag{73}$$

where the water content function is given by:

$$F_w = \left(\frac{\theta}{\theta_b}\right)^B \tag{74}$$

where B is an empirical exponent, and the soil temperature function is given by a numerical approximation of the Arrhenius equation (Boesten & van der Linden, 1991) modified for low soil temperatures:

$$\begin{aligned} F_t &= e^{\alpha (T - T_{ref})} \quad ; \quad T > 5^o C \\ F_t &= \left(\frac{T}{5}\right) e^{\alpha (5 - T_{ref})} \quad ; \quad 0 \le T \le 5^o C \\ F_t &= 0 \quad ; \quad T < 0^o C \end{aligned} \tag{75}$$

where T is the soil temperature, T_{ref} is the temperature at which μ_{ref} is measured and α is a composite parameter dependent on T, T_{ref}, the gas constant and the molar activation energy (Boesten & van der Linden, 1991). Degradation rates in the two flow domains are therefore given by:

$$U_{d(ma)} = c_{ma} \theta_{ma} \mu_{(l)ma} + f \gamma s_{ma} \mu_{(s)ma} \tag{76}$$

$$U_{d(mi)} = c_{mi} \theta_{mi} \mu_{(l)mi} + (1 - f - f_{ne}) \gamma s_{mi} \mu_{(s)mi} \tag{77}$$

where the subscripts l and s refer to liquid and equilibrium adsorbed phases respectively. In the case of tritium, μ is set automatically within the program (equivalent to a half-life of 12.3 years) and is not influenced by either soil moisture or temperature.

If a pesticide metabolite is being simulated, the degraded mass of the parent compound (as a function of both depth and time) is used as a source term in equation 64. A user-defined conversion factor is applied to the degraded mass to account for differences in molecular weight and/or additional parallel metabolic pathways.

6.2. Discretisation of the convection-dispersion equation

From equation 64, an effective retardation coefficient *R* is defined as:

$$R = \gamma\left(1 - f - f_{ne}\right)k_f c^{m-1} \tag{78}$$

Substituting equation 78 into equation 64 and rearranging gives :

$$\frac{\partial(c\theta)}{\partial t} + \frac{\partial(cR)}{\partial t} = \frac{\partial}{\partial z}\left(D\theta\frac{\partial c}{\partial z} - qc\right) - U \tag{79}$$

This form of the convection-dispersion equation is solved using a Crank-Nicholson finite difference scheme. The second term on the left-hand side is expanded as:

$$\frac{\partial}{\partial t}(Rc) \approx \frac{R_i^{n+1}c_i^{n+1} - R_i^n c_i^n}{\Delta t} \tag{80}$$

where R_i^{n+1} is the retardation factor at timestep $n+1$ and the numerical layer i. R_i^{n+1} is unknown for values of the Freundlich exponent, m, that differ from unity. An iterative solution is used where R_i^{n+1} is updated at each iteration step. The iteration stops when:

$$abs\left(c_i^{\tau} - c_i^{\tau+1}\right)/c_i^{\tau} \leq 0.0005 \quad \text{for all } i = 1, 2, 3, \ldots..n \tag{81}$$

where τ is the iteration level and n is the number of numerical soil layers. The convection term $\partial(qc)/\partial z$ is discretised as:

$$\left(\beta_1\frac{q_{i-1/2}}{\Delta z_i}c_{i-1} + \beta_2\frac{q_{i-1/2}}{\Delta z_i}c_i - \beta_3\frac{q_{i+1/2}}{\Delta z_i}c_i - \beta_4\frac{q_{i+1/2}}{\Delta z_i}c_{i+1}\right)^{n+1/2} \tag{82}$$

A fully upstream weighted scheme is used where the weights are defined as β_1=1 and β_2=0 if $q_{i-1/2}$ is positive, β_3=1 and β_4=0 if $q_{i+1/2}$ is positive, β_1=0 and β_2=1 if $q_{i-1/2}$ is negative and β_3=0 and β_4=1 if $q_{i+1/2}$ is negative. This approach minimises 'overshoot' problems and oscillations that may sometimes be encountered in the presence of steep concentration gradients. However, upstream weighting introduces

considerable numerical dispersion, which is minimized by an empirical correction of the effective dispersion:

$$Corr = abs(q)k_{corr} \tag{83}$$

where q is the water flow rate and k_{corr} is a constant. The correction factor $Corr$ is subtracted from the effective dispersion coefficient before solving the convection-dispersion equation. The value of k_{corr} is determined from comparisons with the analytical solution for steady state water flow and a step input of non-adsorbing solutes. If the corrected dispersion coefficient becomes negative, then equation 82 is instead solved with an equal weighting scheme, such that $\beta_1 = \beta_2 = \beta_3 = \beta_4 = 0.5$. This is only likely to occur for extremely small values of the dispersivity.

6.3. Boundary conditions

The solute concentration in water routed into the macropores c_{ma}^{*} is calculated by assuming instantaneous local equilibrium and complete mixing of incoming net precipitation with the water stored in a shallow surface soil layer or "mixing depth", z_d (Steenhuis & Walter, 1980):

$$c_{ma}^{*} = \frac{Q_{d(t-\Delta t)} + (W_s + W_d)c_t}{W_s + W_d + \left(z_d\left(\theta_{mi(m)(1)} + \left((1 - f - f_{ne})\gamma_1 k_{f(1)} c_{mi(t-\Delta t)(1)}^{m-1}\right)\right)\right)} \tag{84}$$

where Q_d is the amount of solute stored in the mixing depth and the subscript *1* refers to the top soil layer. The solute flux into the macropores is then given as the product of I_{ma} and c_{ma}^{*}. The amount of solute added to, or removed from, the micropores in the top layer $Q_{mi(1)}$ is then given by:

$$Q_{mi(1)} = (W_s + W_d)c_t - I_{ma}c_{ma}^{*} \tag{85}$$

For the known hydraulic gradient and the lysimeter bottom boundary conditions for water flow, solute flow out of the bottom layer in the soil profile is calculated assuming zero dispersion. For the remaining bottom boundary condition options for water flow, solute transport at the base of the profile is calculated assuming a constant solute concentration at the bottom boundary (e.g. in the groundwater c_g).

7. Soil temperature

Soil temperatures are calculated by the heat conduction equation :

$$\frac{\partial T}{\partial t} = \frac{1}{C_h}\frac{\partial}{\partial z}\left(k_h \frac{\partial T}{\partial z}\right) \tag{86}$$

where k_h is the thermal conductivity (W m^{-1} K^{-1}) and C_h is the volumetric heat capacity (J m^{-3} K^{-1}), both of which are calculated internally within the program from the known physical properties of the soil:

$$C_h = \left(4.2\times10^6\,\theta\right) + \left(\left(\frac{\gamma}{\gamma_{solid}}\right)w_{\min}\right) \tag{87}$$

where w_{min} is a weighted heat capacity of the soil solids given by:

$$w_{\min} = 2.7\times10^6 f_{om} + 2.0\times10^6\left(1 - f_{om}\right) \tag{88}$$

where f_{om} is the fractional soil organic matter content, and:

$$k_h = A1 + A2\exp\left(\frac{-A3}{100\theta}\right) \tag{89}$$

where the empirical constants $A1$, $A2$ and $A3$ are given by (Hubrechts, 1998):

$$\begin{aligned} A1 &= -0.295 + 1.26 f_{clay} + 0.388\gamma \\ A2 &= -1.776 + 2.0476\gamma + 12.4 f_{oc} \\ A3 &= \exp\left(0.976 + 6.5 f_{clay} + 14 f_{oc}\right) \end{aligned} \tag{90}$$

where f_{clay} and f_{oc} are the fractional clay and organic carbon contents respectively, and the bulk density is given in units of g cm^{-3}.

7.1. Numerical solution

Equation 86 is solved using a standard Crank-Nicholson finite difference scheme where both C_h and k_h are explicitly linearised. The k_h values between nodes are calculated using geometric means.

7.2. Boundary conditions

Boundary conditions for the soil surface and the base of the profile are required to solve equation 86. In the absence of a surface snowpack, the soil surface temperature T_s is approximated by:

$$T_s = \left(\frac{T_{\max} + T_{\min}}{2} \right) + \left[\left(\frac{T_{\max} - T_{\min}}{2} \right) \cos \left(2\pi \left(\frac{t^* - 15}{24} \right) \right) \right] \tag{91}$$

where $T_{\max}$ and $T_{\min}$ are the daily maximum and minimum air temperatures and t^* is the time during the day. With snow cover, the temperature at the soil surface is calculated assuming steady-state heat flow through a snowpack of constant density and thermal conductivity (Jansson, 1991). The bottom boundary condition is given as a temperature T_b predicted from an analytical solution of the heat conduction equation assuming a sinusoidal variation of temperature at the soil surface on an annual basis:

$$T_b = \left(\frac{T_{amax} + T_{amin}}{2} \right) + \left(\frac{T_{amax} - T_{amin}}{2} \right) e^{(-z_l / D_a)} \cos \left[2\pi \left(\left(\frac{D^* - 212}{365} \right) - \left(\frac{z_l}{D_a} \right) \right) \right] \tag{92}$$

where T_{amax} and T_{amin} are the maximum and minimum values of monthly mean air temperature, z_l is the depth of the soil profile and D_a is the penetration depth of the temperature wave (i.e. the depth at which the amplitude of the wave is reduced to e^{-1} of the value at the surface) given by:

$$D_a = \sqrt{\frac{P\, D_h}{\pi}} \tag{93}$$

where P is the cycle duration (i.e. one year) and D_h is a profile-averaged thermal diffusivity ($= k_h/C_h$) calculated assuming $\theta = \theta_b$.

8. Acknowledgements

The development of MACRO5.0 was funded by two EU 5th framework projects: APECOP ('Effective approaches for assessing the predicted environmental concentrations of pesticides', QLK4-CT1999-01238) and PEGASE ('Pesticides in European Groundwater', EVK1-CT1999-00028). We are also grateful to Roy Kasteel and Jan Vanderborght at the Forschungszentrum Jülich (Germany) for their valuable assistance in the development work, by benchmarking Beta versions of the code against a range of analytical solutions for water flow and solute transport problems. We are also grateful to those Beta testers whose efforts have lead to the painstaking eradication of bugs in the code, and insightful suggestions for improving the user interface, especially Peter van der Keur at GEUS (Denmark) and Stefan Reichenberger at the University of Giessen (Germany). Last, but definitely not least, we are indebted to colleagues and students at the Department of Soil Sciences, SLU, who have tested the model against a wide range of field and laboratory experimental data during the last year or two, especially Stephanie Roulier, Fredrik Stenemo, Sven Wahl, Jonathan Fauriel, Guillaume Tamagnan and Johan Strömqvist.

9. References

Altfelder, S., Streck, T. & Richter, J. 2000. Nonsingular sorption of organic compounds in soil: the role of slow kinetics. *Journal of Environmental Quality 29*, 917-925.

Beven, K. & Germann, P. 1982. Macropores and water flow in soils. *Water Resources Research 18*, 1311-1325.

Boesten, J.J.T.I. & van der Linden, A.M.A. 1991. Modeling the influence of sorption and transformation on pesticide leaching and persistence. *Journal of Environmental Quality 20*, 425-435.

Booltink, H.W.G., Hatano, R. & Bouma, J. 1993. Measurement and simulation of bypass flow in a structured clay soil : a physico-morphological approach. *Journal of Hydrology 148*, 149-168.

Brown, C.D., Marshall, V., Deas, A., Carter, A.D., Arnold, D. & Jones, R.L. 1999. Investigation into the effect of tillage on solute movement to drains through a heavy clay soil. II. Interpretation using a radio-scanning technique, dye tracing and modelling. *Soil Use & Management 15*, 94-100.

Carsel, R.F., Smith, C.N., Mulkey, L.A., Dean, J.D. & Jowise, P. 1984. *Users manual for the pesticide root zone model (PRZM).* EPA-600/3-84-109, E.P.A. Athens, Georgia, U.S.A., 216 pp.

Celia, M.A, Bouloutas, E.T. & Zarba, R.L. 1990. A general mass conservative numerical solution for the unsaturated flow equation. *Water Resources Research 26*, 1483-1496.

Choudhury, B.J. & Monteith, J.L. 1988. A four-layer model for the heat budget of homogeneous land surfaces. *Quarterly Journal of the Royal Meteorological Society 114*, 373-398.

Clothier, B.E. & Smettem, K.R.J. 1990. Combining laboratory and field measurements to define the hydraulic properties of soil. *Soil Science Society of America Journal 54*, 299-304.

Feddes, R.A., Bresler, E. & Neuman, S.P. 1974. Field test of a modified numerical model for water uptake by root systems. *Water Resources Research 10*, 1199-1206.

Feddes, R.A., Kowalik, P., Kolinska-Malinka, K. & Zaradny, H. 1976. Simulation of field water uptake by plants using a soil water dependent root extraction function. *Journal of Hydrology 31*, 13-26.

Flury, M., Flühler, H., Jury, W.A. & Leuenberger, J. 1994. Susceptibility of soils to preferential flow of water. *Water Resources Research 30*, 1945-1954.

Flury M. 1996. Experimental evidence of transport of pesticides through field soils – a review. *Journal of Environmental Quality 25*, 25-45.

FOCUS, 1995. The final report of the work of the regulatory modeling work group of FOCUS (FOrum for the Coordination of pesticide fate models and their Use), *EU Doc. 4952/VI/95*, 123 pp.

Gerke, H.H. & van Genuchten, M.T. 1993. Evaluation of a first-order water transfer term for variably-saturated dual-porosity flow models. *Water Resources Research 29*, 1225-1238.

Gerke, H.H. & van Genuchten, M.T. 1996. Macroscopic representation of structural geometry for simulating water and solute movement in dual-porosity media. *Advances in Water Resources 19*, 343-357.

Gerke, H.H. & Köhne, J.M. 2002. Estimating hydraulic properties of soil aggregate skins from sorptivity and water retention. *Soil Science Society of America Journal*, *66*, 26-36.

Germann, P. 1985. Kinematic wave approach to infiltration and drainage into and from soil macropores. *Transactions of the ASAE 28*, 745-749.

Gerwitz, A. & Page, E.R. 1974. An empirical mathematical model to describe plant root systems. *Journal of Applied Ecology 11*, 773-780.

Hoffmann-Riem, H., van Genuchten, M.T. & Flühler, H. 1999. General model for the hydraulic conductivity of unsaturated soils. In: *Characterization and measurement of the hydraulic properties of unsaturated porous media*, ed. M.T. van Genuchten; F.J. Leij; L. Wu, pp. 31-42, Univ. California, Riverside, CA, U.S.A.

Hooghoudt, S.B. 1940. Bijdrage tot de kennis van enige natuurkundige grootheden van der grond. *Verslagen van Landbouwkundige Onderzoekingen 46*, 515-707 (in Dutch).

Hubrechts, L. 1998. Transfer functions for the generation of thermal properties of Belgian soils. Dissertationes de Agricultura 372, PhD thesis, Catholic University of Leuven, Belgium, 107 pp.

Jansson, P.-E. 1991. Simulation model for soil water and heat conditions. Description of the SOIL model. *Report 165, Div. of Agric. Hydrotechn., Dept. Soil Sci., Swedish Univ. Agric. Sci., Uppsala*, 72 pp.

Jarvis, N.J. 1989. A simple empirical model of root water uptake. *Journal of Hydrology 107*, 57-72.

Jarvis, N.J. 1991. MACRO - A model of water movement and solute transport in macroporous soils. *Reports and Dissertations 9, Dept. Soil Sci., Swedish Univ. Agric. Sci., Uppsala*, 58 pp.

Jarvis, N.J., Jansson, P-E., Dik, P.E. & Messing, I. 1991. Modelling water and solute transport in macroporous soil. I. Model description and sensitivity analysis. *Journal of Soil Science 42*, 59-70.

Jarvis, N.J. 1994. The MACRO model (Version 3.1). Technical description and sample simulations. *Reports and Dissertations 19, Dept. Soil Sci., Swedish Univ. Agric. Sci., Uppsala*, 51 pp.

Jarvis, N.J. & Messing, I. 1995. Near-saturated hydraulic conductivity in soils of contrasting texture as measured by tension infiltrometers. *Soil Science Society America Journal 59*, 27-34.

Jarvis N. J. 1998. Modelling the impact of preferential flow on non-point source pollution. In: *Physical non-equilibrium in soils: modeling and application*, ed. H H Selim; L Ma, pp. 195-221, Ann Arbor Press, Chelsea, MI, U.S.A.

Jarvis, N.J., Brown, C.D. & Granitza, E. 2000. Sources of error in model predictions of pesticide leaching: a case study using the MACRO model. *Agricultural Water Management 44*, 247-262.

Jarvis, N.J. 2002. Macropore and preferential flow. In: *The Encyclopedia of Agrochemicals*, (ed. J. Plimmer), vol.3, 1005-1013, J. Wiley & Sons, Inc.

Kladivko, E.J., van Scoyoc, G.E., Monke, E.J., Oates, K.M. & Pask, W. 1991. Pesticide and nutrient movement into subsurface tile drains on a silt loam soil in Indiana. *Journal of Environmental Quality 20*, 264-270.

Kätterer, T., Schmied, B., Abbaspour, K.C. & Schulin, R. 2001. Single- and dual-porosity modelling of multiple tracer transport through soil columns: effects of initial moisture and mode of application. *European Journal of Soil Science 52*, 25-36.

Kung, K-J. S. 1990. Preferential flow in a sandy vadose zone: 1. Field observation. *Geoderma 46*, 51-58.

Larsson, M.H. & Jarvis, N.J. 1999a. Evaluation of a dual-porosity model to predict field-scale solute transport in macroporous soil. *Journal of Hydrology 215*, 153-171.

Larsson, M.H. & Jarvis, N.J. 1999b. A dual-porosity model to quantify macropore flow effects on nitrate leaching. *Journal of Environmental Quality 28*, 1298-1307.

Larsson, M.H. & Jarvis, N.J. 2000. Quantifying interactions between compound properties and macropore flow effects on pesticide leaching. *Pest Management Science 56*, 133-141.

Leeds-Harrison, P.B., Shipway, C.J.P., Jarvis, N.J. & Youngs, E.G. 1986. The influence of soil macroporosity on water retention, transmission and drainage in a clay soil. *Soil Use and Management 2*, 47-50.

Lindroth, A. 1985. Canopy conductance of coniferous forests related to climate. *Water Resources Research 21*, 297-304.

Luckner, L., van Genuchten, M.T. & Nielsen, D.R. 1989. A consistent set of parametric models for the two-phase flow of immiscible fluids in the subsurface. *Water Resources Research 25*, 2187-2193.

Messing, I. & Jarvis, N.J. 1990. Seasonal variations in field-saturated hydraulic conductivity in two swelling clay soils in Sweden. *Journal of Soil Science 41*, 229-237.

Miller, E.E. & Miller, R.D. 1956. Physical theory for capillary flow phenomena. *Journal of Applied Physics 27*, 324-332.

Millington, R.J. & Quirk, J.P. 1961. Permeability of porous solids. *Transactions of the Faraday Society 57*, 1200-1207.

Mohanty, B., Bowman, R.S., Hendrickx, J.M.H. & van Genuchten, M.T. 1997. New piecewise-continuous hydraulic functions for modeling preferential flow in an intermittent flood-irrigated field. *Water Resources Research 33*, 2049-2063.

Monteith, J.L. 1965. *Evaporation and environment*. In: G.E. Fogg (ed.) The state and movement of water in living organisms, 19th Symp. Soc. Exp. Biol., 205-234.

Mualem, Y. 1976. A new model for predicting the hydraulic conductivity of unsaturated porous media. *Water Resources Research 12*, 513-522.

Nieber, J.L. 1996. Modeling finger development and persistence in initially dry porous media. *Geoderma, 70*, 207-229.

Ray, C., Ellsworth T.R., Valocchi, A.J. & Boast, C.W. 1997. An improved dual-porosity model for chemical transport in macroporous soils. *Journal of Hydrology 193*, 270-292.

Ritsema, C.J., Dekker, L.W., Hendrickx, J.M.H. & Hamminga, W. 1993. Preferential flow mechanism in a water repellent sandy soil. *Water Resources Research 29*, 2183-2193.

Rojas K.W. & Ahuja L.R. 1999. Management practices. In: Ahuja L.R., Rojas K.W., Hanson, J.D, Shaffer M.J, Ma, L. (eds) Root Zone Water Quality Model, Modelling management effects on water quality and crop production. Water Resources Publications, LLC, Highlands Ranch, Colorado, pp 245-280.

Šimůnek, J., Jarvis, N.J., van Genuchten, M.T. & Gärdenäs, A. 2003. Review and comparison of models for describing nonequilibrium and preferential flow and transport in the vadose zone. *Journal of Hydrology*, *272*, 14-35.

Steenhuis, T.S. & Walter, M.F. 1980. Closed form solution for pesticide loss in runoff water. *Transactions of the ASAE 23*, 615-620, 628.

Steenhuis, T.S. & Parlange, J.-Y. 1991. Preferential flow in structured and sandy soils. In *Proceedings of the National Symposium on Preferential Flow*. (eds. T. Gish & A. Shirmohammadi), ASAE, St. Joseph, MI, U.S.A., 12-21.

van Dam J.C. 2000. Field-scale water flow and solute transport. SWAP model concepts, parameter estimation and case studies. *PhD thesis, Wageningen University, Wageningen, Netherlands*, 167p.

van Genuchten, M.T. 1980. A closed-form equation for predicting the hydraulic conductivity of unsaturated soils. *Soil Science Society of America Journal 44*, 892-898.

van Genuchten, M.T. 1985. A general approach for modeling solute transport in structured soils. In *Proceedings 17th International Congress IAH, Hydrogeology of rocks of low permeability.* Memoires IAH, 17, 513-526.

van Genuchten, M.T. & Dalton, F.N. 1986. Models for simulating salt movement in aggregated field soils. *Geoderma 38*, 165-183.

Villholth, K.G. & Jensen, K.H. 1998. Flow and transport processes in a macroporous subsurface-drained glacial till soil. II: Model analysis. *Journal of Hydrology 207*, 121-135.

Vogel T., van Genuchten M.T. & Cislerova, M. 2001. Effect of the shape of the soil hydraulic functions near saturation on variably-saturated flow predictions. *Advances in Water Resources 24*, 133-144.

Williams R.R., Jones, C.A., Dyke P.T. 1984. A modeling approach to determining the relationship between erosion and soil productivity. *Trans. ASAE*, 27, 129-142.

Wilson, G.V., Jardine, P.M. & Gwo, J.P. 1992. Modeling the hydraulic properties of a multiregion soil. *Soil Science Society of America Journal*, *56*, 1731-1737.

Youngs, E.G. 1980. The analysis of groundwater seepage in heterogeneous aquifers. *Hydrological Sciences Bulletin 25*, 155-165.

List of symbols

α_f	Attenuation factor for radiation interception (-)
A_d	Drainage area (L^2)
A_f	Shape factor (L^{-2})
A_{ne}	Amount of solute kinetically sorbed (whole-soil volume basis) ($M\ L^{-2}$)
A1	Empirical constant (-)
A2	Empirical constant (-)
A3	Empirical constant (-)
B	Empirical exponent (-)
c	Solute concentration in soil solution ($M\ L^{-3}$)
c_g	Solute concentration in groundwater ($M\ L^{-3}$)
c_f	Correction factor (-)
c_{ma}	Solute concentration in macropores ($M\ L^{-3}$)
c_{ma}^*	Solute concentration in water flow into macropores at soil surface ($M\ L^{-3}$)
c_{mi}	Solute concentration in micropores ($M\ L^{-3}$)
c_p	Solute concentration in precipitation ($M\ L^{-3}$)
c_t	Solute concentration in net rainfall ($M\ L^{-3}$)
c'	Solute concentration (in macropores or micropores) ($M\ L^{-3}$)
C	Differential water capacity (L^{-1})
C_h	Volumetric heat capacity ($J\ L^{-3}\ {}^oC^{-1}$)
C_{init}	Parameter controlling initial consolidation state (%)
C_p	Specific heat capacity of air ($J\ M^{-1}\ {}^oC^{-1}$)
C_{ma}	Macropore air content ($L^3\ L^{-3}$)
d	Effective diffusion pathlength (L)
d_h	Displacement height (L)
d_z	Equivalent soil depth (L)
D	Dispersion coefficient ($L^2\ T^{-1}$)
D^*	Julian day number (-)
D_a	Penetration depth of the soil temperature wave (L)
D_e	Effective diffusion coefficient ($L^2\ T^{-1}$)
D_h	Profile-average thermal diffusivity ($L^2\ T^{-1}$)
D_{harv}	Day of harvest (-)
D_{max}	Day of maximum leaf area (-)
D_{min}	Day number specifying the end of an initial linear growth phase (-)
D_o	Diffusion coefficient in free water ($L^2\ T^{-1}$)
D_v	Dispersivity (L)
D_w	Effective water diffusivity ($L^2\ T^{-1}$)
D_z	Soil depth between drains and the base of the profile (L)
$D_{\theta b}$	Water diffusivity at micropore saturation ($L^2\ T^{-1}$)

$D_{\theta mi}$	Water diffusivity in the micropores ($L^2\ T^{-1}$)
e	Seepage potential in a saturated domain ($L^3\ T^{-1}$)
e_{ma}	Macroporosity ($L^3\ L^{-3}$)
$e_{mi(tilled)}$	Microporosity in a tilled soil ($L^3\ L^{-3}$)
$e_{mi(cons)}$	Microporosity in a fully consolidated soil ($L^3\ L^{-3}$)
e_s	Minimum macroporosity in fully swollen soil ($L^3\ L^{-3}$)
e_{mi}	Microporosity ($L^3\ L^{-3}$)
E	Seepage potential in a saturated zone ($L^3\ T^{-1}$)
E_a	Actual transpiration ($L\ T^{-1}$)
E_p	Potential `dry-canopy' transpiration ($L\ T^{-1}$)
$E_{p(soil)}$	Potential soil evaporation ($L\ T^{-1}$)
E_r	Potential root water uptake ($L\ T^{-1}$)
E_s	Soil evaporation ($L\ T^{-1}$)
E_{wp}	Potential wet canopy evaporation ($L\ T^{-1}$)
f	Fraction of sorption sites in the macropores (-)
f_c	Concentration factor for solute uptake (-)
f_{clay}	Fractional clay content (-)
f_e	Foliar washoff coefficient (L^{-1})
f_{ne}	Fraction of kinetic adsorption sites (-)
f_{oc}	Fractional organic carbon content (-)
f_{om}	Fractional organic matter content (-)
f^*	Impedance factor (-)
F_{crop}	Fraction of radiation intercepted by (green) crop surfaces
F_{soil}	Fraction of radiation reaching the soil
F_t	Soil temperature function (-)
F_w	Soil water function (-)
G_f	Geometry factor (-)
$GLAI$	Green leaf area index (-)
$GLAI_{harv}$	Green leaf area index at harvest (-)
$GLAI_{max}$	Maximum green leaf area index (-)
$GLAI_{min}$	Minimum green leaf area index (-)
h	Height (L)
h_l	Height at the bottom of a layer (L)
h_u	Height at the top of a layer (L)
h_0	Height at the base of a saturated zone (L)
H	Water table height (L)
H_c	Crop height (L)
I	Tillage intensity factor
I_{ma}	Macropore infiltration (L)
I_{mi}	Micropore infiltration (L)

I_{max}	Infiltration capacity (L)
k_{corr}	Empirical correction factor (L)
k_{cons}	Consolidation rate constant (L^{-1})
k_f	Freundlich sorption coefficient ($L^3 M^{-1}$)
k_h	Thermal conductivity ($J L^{-1} T^{-1} {}^oC^{-1}$)
k_0	Coefficient of proportionality ($L^3 T^{-1}$)
k_s	Stomatal conductance ($L T^{-1}$)
$k_{s(max)}$	Maximum stomatal conductance ($L T^{-1}$)
K	Hydraulic conductivity ($L T^{-1}$)
K_b	Saturated micropore hydraulic conductivity ($L T^{-1}$)
$K_{b(cons)}$	Saturated micropore hydraulic conductivity in consolidated soil ($L T^{-1}$)
K_{ma}	Hydraulic conductivity (macropores) ($L T^{-1}$)
K_{mi}	Hydraulic conductivity (micropores) ($L T^{-1}$)
K_s	Saturated hydraulic conductivity ($L T^{-1}$)
$K_{s(ma)}$	Saturated hydraulic conductivity in macropores ($L T^{-1}$)
$K_{s(cons)}$	Saturated hydraulic conductivity in fully consolidated soil ($L T^{-1}$)
$K_{s(min)}$	Saturated hydraulic conductivity in fully swollen soil ($L T^{-1}$)
K^*_s	'Fictitious' saturated hydraulic conductivity ($L T^{-1}$)
l	Tortuosity factor (micropores) (-)
L	Drain spacing (L)
LAI	Total leaf area index (-)
m	Exponent in the Freundlich sorption isotherm (-)
m_{vg}	Shape parameter in the van Genuchten water retention function (-)
m^*	Empirical exponent (-)
n^*	Pore size distribution index (macropores) (-)
n^*_{tilled}	Maximum pore size distribution index (macropores, tilled soil) (-)
n_{vg}	Shape parameter in the van Genuchten water retention function (-)
p	Slope of the shrinkage characteristic (-)
P	Cycle duration of the soil temperature wave (T)
q	Water flux ($L T^{-1}$)
q_{const}	Parameter regulating water outflow at bottom boundary (T^{-1})
q_d	Drainage rate above drain depth ($L T^{-1}$)
$q_{d(tot)}$	Total drainage from a saturated zone ($L T^{-1}$)
q_{dd}	Drainage rate below drain depth ($L T^{-1}$)
q_{max}	Maximum possible water flux to the soil surface ($L T^{-1}$)
q_{out}	Percolation rate at bottom boundary ($L T^{-1}$)
Q_c	Canopy storage of solute ($M L^{-2}$)
Q_d	Store of solute in the mixing depth ($M L^{-2}$)
Q_{mi}	Solute store in micropores ($M L^{-2}$)
r	Fractional root length (-)

r_c	Crop surface resistance (T L^{-1})
r_{ss}	Aerodynamic resistance, soil to canopy (T L^{-1})
r_{ca}	Aerodynamic resistance, canopy to air (T L^{-1})
R	Retardation coefficient (-)
R_{amount}	Rainfall amount (L)
R_b	Outgoing long-wave radiation (J L^{-2} T^{-1})
R_i	Incoming solar radiation (J L^{-2} T^{-1})
R_n	Net radiation (J L^{-2} T^{-1})
R_t	Retention time for solute in the saturated zone (T)
s	Solute concentration in the solid phase (M M^{-1})
s_{ma}	Solute concentration in the solid phase, macropores (M M^{-1})
s_{mi}	Solute concentration in the solid phase, micropores (M M^{-1})
S	Effective water content (L^3 L^{-3})
S_i	Source-sink term (T^{-1})
S_{ma}	Degree of saturation in the macropores (L^3 L^{-3})
$S_{mi(\theta b)}$	Effective water content at micropore saturation (L^3 L^{-3})
S_r	Root water uptake sink (T^{-1})
S_w	Source/sink term, exchange of water between domains (T^{-1})
t	Time (T)
t^*	Time during the day (T)
T	Soil temperature (^oC)
T_{amax}	Maximum monthly mean air temperature (^oC)
T_{amin}	Minimum monthly mean air temperature (^oC)
T_b	Temperature at the base of the soil profile (^oC)
T_{max}	Daily maximum air temperature (^oC)
T_{min}	Daily minimum air temperature (^oC)
T_{ref}	Reference temperature (^oC)
T_s	Soil surface temperature (^oC)
U_i	Source-sink term (M L^{-3} T^{-1})
U_g	Solute loss/gain in lateral groundwater flow (M L^{-3} T^{-1})
U_c	Sink term, solute uptake by crop (M L^{-3} T^{-1})
U_d	Sink term, biodegradation (M L^{-3} T^{-1})
U_e	Solute exchange between flow domains (M L^{-3} T^{-1})
U_t	Sink term, leaching to drains/groundwater seepage (M L^{-3} T^{-1})
u	Wind speed (L T^{-1})
u_p	Wetted drain perimeter (L)
v	Pore water velocity (L T^{-1})
VPD	Vapour pressure deficit (M L^{-1} T^{-2})
VPD_{50}	Vapour pressure deficit at which stomatal conductance is reduced to 50% of the maximum value (M L^{-1} T^{-2})

w_{min}	Weighted thermal conductivity of the solid fraction (J m^{-1} K^{-1})
W_c	Canopy storage of water (L)
W_d	Drip throughfall (L)
W_i	Canopy interception (L)
W_s	Direct throughfall (L)
x_1	Empirical exponent (-)
x_2	Empirical exponent (-)
z	Depth or height (L)
z_d	Mixing depth (L)
z_l	Depth of the soil profile (L)
z_m	Depth of the mid-point of a layer (L)
z_o	Roughness length (L)
z_r	Root depth (L)
z_b	Distance between the bottom of the soil profile and the centre of a numerical layer (L)

α	Exponent in temperature response function (T^{-1})
α_k	Mass transfer coefficient (kinetic sorption) (T^{-1})
α_r	Albedo (-)
α_{vg}	Shape parameter in the van Genuchten water retention function (L^{-1})
$\alpha_{vg(tilled)}$	Maximum van Genuchten α parameter (L^{-1})
β	Weighting factor (-)
ε	Porosity (L^3 L^{-3})
γ	Soil bulk density (M L^{-3})
γ_{cons}	Bulk density in consolidated soil (M L^{-3})
γ_{init}	Initial bulk density (M L^{-3})
γ_{solid}	Particle density (M L^{-3})
γ_{tilled}	Minimum bulk density (M L^{-3})
γ_c	Pyschrometric constant (M L^{-1} T^{-2} $^oC^{-1}$)
γ_w	Scaling factor (-)
Δ	Slope of the saturation vapour pressure/temperature curve (M L^{-1} T^{-2} $^oC^{-1}$)
Δt	Time step (T)
Δz	Layer thickness (L)
ζ	Root distribution parameter (-)
θ	Water content (L^3 L^{-3})
θ_b	Saturated micropore water content (L^3 L^{-3})
θ_{ma}	Macropore water content (L^3 L^{-3})
θ_{max}	Maximum water content in micropores (L^3 L^{-3})
θ_{mi}	Micropore water content (L^3 L^{-3})

$\theta_{mi(m)}$	Mobile water content in micropores ($L^3\ L^{-3}$)
θ_r	Residual water content ($L^3\ L^{-3}$)
θ_s	Saturated water content ($L^3\ L^{-3}$)
θ^*_s	Fictitious saturated water content ($L^3\ L^{-3}$)
θ_w	Extractable water content (wilting point) ($L^3\ L^{-3}$)
ρ	Density of air ($M\ L^{-3}$)
λ_v	Latent heat of vapourization ($J\ M^{-1}$)
μ	Degradation rate coefficient (soil) (T^{-1})
μ_c	Canopy dissipation rate coefficient (T^{-1})
μ_{ref}	Reference degradation rate coefficient (soil) (T^{-1})
ψ	Soil water pressure head (L)
ψ_{max}	Maximum soil water pressure head (micropores) (L)
ψ_b	Boundary soil water pressure head (L)
$\psi_{surface}$	Pressure head at the soil surface (L)
ω	Water stress reduction factor (-)
ω^*	Water stress index (-)
ω^*_c	Root adaptability factor (-)

List of publications in Emergo

2003:1 Holmberg, H. Metodutveckling för utvärdering av simuleringsmodeller med hjälp av fluorescerande ämnen (Development of methods to evaluate simulation models using fluorescent dye tracers). M.Sc. thesis. 50 pages.

2003:2 Olsson, C. Översvämningsåtgärder i Emån- simulering i Mike 11 modellen (Effects of proposed embankments along the river Emån- Simulation in the Mike 11 model). M.Sc. thesis. 34 pages.

2003:3 Gärdenäs, A. Eckersten, H. & Lillemägi, M. Modeling long-term effects of N fertilization and N deposition on the N balance of forest stands in Sweden. 30 pages.

2003:4 Jarvis, N. Hanze, K. Larsbo, M. Stenemo, F. Persson, L. Roulier, S. Alavi, G. Gärdenäs, A. Rönngren, J. Scenario development and parameterization for pesticide exposure assessments for Swedish groundwater. 26 pages. ISBN: 91-576-6588-5

2003:5 Eckersten, H., Gärdenäs, A. & Lewan, E. (Eds.) Biogeofysik – en introduktion (Environmental physics – an introduction). 141 pages. ISBN: 91-576-6591-5

2003:6 Larsbo, M & Jarvis, N. MACRO5.0. A model of water flow and solute transport in macroporous soil. Technical description. 48 pages. ISBN: 91-576-6592-3